Identification of Control-Relevant Diesel Engine Models Using a Local Linear Parametric Approach [*]

Thijs van Keulen [*,**] **Lars Huijben** [*,**] **Tom Oomen** [*]

[*] *Eindhoven University of Technology, Control Systems Technology group, Eindhoven, the Netherlands (e-mail: t.a.c.v.keulen@tue.nl)*
[**] *DAF Trucks N.V., Eindhoven, the Netherlands*

Abstract: Control is essential to meet future emission requirements in combustion engines. Accurate models are required to design a controller that achieves robust performance over a range of operating conditions. The aim of this paper is to develop a non-parametric and parametric identification procedure that is specifically tailored towards high performance diesel engine control, while minimizing measurement time. First, a non-parametric identification is proposed where the inputs are excited with multisines. A Local Rational Method (LRM) is employed to obtain multivariable Frequency Response Functions (FRFs) in a single experiment. Secondly, a parametric identification procedure uses the non-parametric estimates to obtain control-relevant parametric models. The identification procedure is demonstrated using a modern Heavy-Duty Diesel (HDD) engine providing highly accurate low order parametric models for a 2x2 plant using just 300s of measurement time at an engine operating point.

Keywords: Engine modelling and control, Automotive system identification and modelling, Frequency domain identification, Identification for control, Automotive sensors and actuators

1. INTRODUCTION

To meet global CO_2 reduction targets without compromising the current efficiency of road transport and complying with the stringent emission legislation, vehicles require a strong reduction of greenhouse gasses. To achieve limits of performance, additional sensors and actuators are being explored. This includes, e.g., Variable Geometry Turbocharging (VGT) and Exhaust Gas Recirculation (EGR). Typical sensor information includes pressure and temperature of the intake and exhaust manifold, NO_x and oxygen concentration in the exhaust, EGR mass flow and turbine speed. The input-output relations depend nonlinearly on operation conditions such as engine speed, load and ambient conditions. Besides, production tolerances, sensor bias, aging and fouling gives uncertainty in the dynamic response of the system. Hence, manual controller tuning becomes prohivitive and time-consuming. As a result, advanced model-based control techniques that can deal with calibration, nonlinearity, uncertainty and constraints in a structured way are promoted by many engine control researchers to fully utilize the engine capabilities and to reduce calibration time.

Many important contributions have been made for advanced control of Heavy-Duty Diesel (HDD) engines, see, e.g., Stewart et al. (2010); Karlsson et al. (2010); Wang et al. (2011); Broomhead et al. (2014). All these strategies rely on parametric system descriptions. However, the modeling and control aspects are typically considered separately. Hence, there is the need for control-relevant HDD engine models. Where control-relevant refers to accurate identification of control-relevant frequency regions, typically around the bandwidth of the closed loop system, and the explicit inclusion of model uncertainty.

One approach to obtain a parametric system description, is to use physical modeling of HDD engines. To limit complexity, models are often reduced to cycle-averaged dynamics (Calendini and Breuer, 2010; Eriksson and Nielson, 2014). Furthermore, model reduction techniques can be applied (Sharma et al., 2011). However, these simplifications significantly decrease the prediction capabilities due to the decrease in temporal and spatial resolution (Guardiola et al., 2012). Moreover, first principle models are generally identified using prediction error identification. Analysis of the model quality in view of robust control may therefore be limited to situations where the system is in the model set (Gevers et al., 2003).

Another approach is to fit a parametric model directly on measurement data. Identification of multivariable local linear models, also in the presence of nonlinearity (Schoukens et al., 2016), is a well established research topic. In Criens et al. (2016) a nonlinear distortion analysis demonstrated that it is safe to use a local linear system approach for HDD engines. Identification of local dynamics of the HDD engine application, is persued by serveral researchers (Henningsson et al., 2012; Isermann, 2014). These approaches do not enforce control-relevant accuracy or provide uncertainty information.

Hence, although important progress on modeling and control of HDD has been made, at present, identification of HDD for control is time consuming and nonoptimal. The aim of this paper is to develop a non-parametric and parametric identification procedure that is specifically tailored towards high performance HDD control, while minimizing measurement time.

Recently, time efficient multivariable local parametric approaches are developed for Frequency Response Functions (FRF) measurements, see McKelvey and Guérin (2012). The Local Rational Method (LRM) provides multivariable FRFs obtained in a single experiment. This yields a mea-
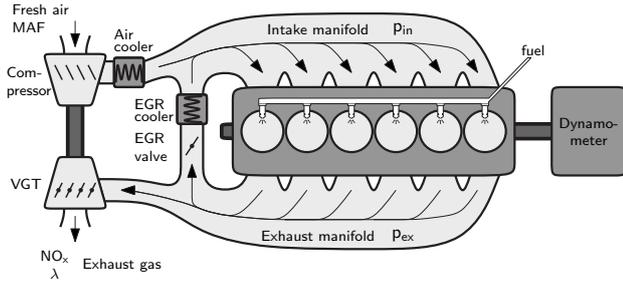

Fig. 1. Schematic engine layout Criens et al. (2015).

surement time reduction of a factor N_u (the number of inputs) with respect to regular multivariable identification techniques. This practicality is of significant importance as measurement time is limited and there are many operating points of the engine for which an estimation is required.

The FRF measurements can be followed by a local linear parametric model fit. In Oomen et al. (2014) an identification algorithm is developed that delivers a system model in terms of recently developed coprime factorizations and thereby extends classical iterative procedures to the closed-loop case. These coprime factorizations have important advantages for uncertainty modeling and robust controller synthesis of complex systems.

The main contributions of this paper are; 1) a highly accurate and fast multivariable FRF measurements of HDD engines using the LRM, 2) development of a frequency based fit procedure leading to control-relevant local linear parametric models of HDD engines, 3) an experimental study providing a comparison of the LRM and parametric fit with a higly accurate plant estimate based on the robust Best Linear Approximation (BLA).

2. SYSTEM DESCRIPTION

A schematic overview of the layout of a typical HDD engine is depicted in Fig. 1. All modern HDD engines apply turbocharging, where the exhaust gas enthalphy is used to boost the fresh air flow. Part of the exhaust gas is redirected to the intake manifold which is known as EGR. Increasing the EGR mass flow will decrease the NO_x formation. However, EGR negatively affects the pumping losses (difference between intake and exhaust manifold pressure) and reduces the exhaust heat available for the turbocharger and hence the fresh air mass flow. Both effects can compromize the fuel efficiency.

The HDD engine design in Fig. 1 comprises a VGT and EGR valve. The EGR valve and the VGT position enable control over the EGR mass flow, and hence the trade-off between fuel consumption and engine out emissions. Since fuel consumption cannot be directly measured, the selection of output signals is not straightforward. This paper aims to provide an identification procedure applicable for any suggested combination of output signals. Hence, two typical HDD sensor signals; exhaust manifold pressure p_{ex} and NO_x concentration, are used to demonstrate the modeling capabilities.

3. NON PARAMETRIC IDENTIFICATION

3.1 Input signal design

Multisine excitation signals are considered to excite the system since they have some advantageous properties. Due to the periodic nature of a multisine, leakage of excitation power to frequencies outside the Discrete Fourier Transform (DFT) window can be completely avoided. Furthermore, because the power in a multisine is concentrated in a limited number of frequencies, the power per frequency is high compared to a signal which excites every frequency resulting in a higher Signal-to-Noise Ratio (SNR). Moreover, the unexcited frequency lines can be used to quantify the nonlinear distortions (Pintelon and Schoukens, 2012, Section 4.2). Finally, random phase multisine signals enable a fast identification for MIMO systems as will be discussed in detail in Section 3.3.

A realisation of a multisine signal is defined as:

$$u(t) = \sum_{k=1}^{N_k} A_k \sin(2\pi f_k t + \varphi_k). \quad (1)$$

With N_k the number of harmonics that are present in the multisine and A_k, f_k and φ_k the respective amplitude, frequency and phase of the k-th sinusoid. The selection of N_k, A_k, f_k and φ_k requires a careful consideration.

For this application, the closed loop control bandwidth is expected to be in the order of 10^{-1} Hz. The frequency range of interest has accordingly been chosen as $f_k \in [0.01, 10]$ Hz. Hence, the period length of the multisine must be at least a 100 s. Sampling occurs with 50 Hz, thus aliasing is not an issue for the highest excitation frequency. Furthermore, the frequency spectrum of the input signal is chosen to be quasi-logarithmic. This spectrum is formed by shifting frequencies of a true logarithmic distribution onto the nearest odd frequency in the DFT grid. Only odd frequencies are excited such that even nonlinearities do not disturb the FRF measurement. A total of $N_k = 35$ harmonics are used as this provides a good trade-off between resolution and input power per frequency. A random phase multisine is considered since it has a reasonable crest factor. Finally, the chosen amplitude spectrum is flat and scaled such that the multisine has a peak value in the range of 10% of the actuator range.

3.2 Multivariable identification techniques

The identification procedure for multiple-input multiple-output (MIMO) systems, is more involved than for single-input single-output (SISO) systems. This is due to the amount of elements that need to be identified. A plant with N_u inputs and N_y outputs will contain $N_y N_u$ elements:

$$\underline{Y}(k) = \underline{G}(f_k)\underline{U}(k), \quad (2)$$

in which $\underline{U}(k) \in \mathbb{R}^{N_u \times 1}$ and $\underline{Y}(k) \in \mathbb{R}^{N_y \times 1}$ the DFT vector of the input and output signals at frequency bin k respectively and $\underline{G}(f_k)$ the plant response at the corresponding frequency. The plant can be identified by rewriting (2) into the form:

$$\underline{G}(f_k) = \underline{Y}(k)\underline{U}(k)^{-1}. \quad (3)$$

Which is only possible if $\underline{U}(k)$ is invertible. This operation yields N_y equations with N_u unknowns per equation.

One approach for the full identification of $\underline{G}$ is to perform N_u experiments. For this purpose, $\underline{Y}(k)$ and $\underline{U}(k)$ are extended by concatenating columns of N_u different experiments, such that $\underline{U}(k) \in \mathbb{R}^{N_u \times N_u}$ and $\underline{Y}(k) \in \mathbb{R}^{N_y \times N_u}$. With this extension, $\underline{U}(k)$ becomes invertible and the multiplication given in (3) results in $N_y N_u$ uniquely identified elements of $\underline{G}$.

By averaging multiple estimates of the plant, a high quality estimate can be created such that it can serve as a bench-

mark for the fast identification method presented in the next section. In a nonlinear setting, the effect of nonlinear distorations can be averaged out by measuring different realisations of the multisine. The linear approximation that is closest to the averaged estimates is denoted as the robust BLA. A detailed description of the robust BLA can be found in Pintelon and Schoukens (2012).

3.3 Fast identification with the local rational method

Another approach is the LRM (McKelvey and Guérin, 2012) which is an identification technique wherein the FRFs are locally approximated by a rational function at every excited frequency. Moreover, specifically the 'fast' method adaption of the LRM is considered as it requires only a single experiment for a full identification of the MIMO plant.

The key idea behind the LRM is to obtain the required additional data (essentially to solve (3)) from a set of $2r_E$ adjoining excited frequencies that surround k. Under the assumption that the underlying system P can be described with a smooth function of frequency, every transfer in P can locally be approximated by a parametric function. Fitting such a local parametric function, in the LRM case consisting of a polynomial numerator and denominator, on every transfer in P in a least squares way on the window $k + r_E$, can be rewritten as a problem consisting of a set of linear equations.

The size of this problem grows with the amount of inputs, outputs, and the complexity of the function that is used to locally approximate P. The number of equations that are available to solve it is equal to the number of excited frequencies in the window $(2r_E + 1)$. Crucially, the data at the considered frequency bins in the window, as well as for different inputs, is uncorrelated due to the use of uncorrelated random phase multisines. If the set of equations is solved, a least squares fit of the local parametric function on the domain of the window is obtained for every transfer in P. This yields an estimate of the elements in P at frequency k.

Since, the response of every excited frequency is approximated by a least squares fit of a rational function through a set of adjacent excited frequencies, it must be assumed that all the system elements are a smooth function of the frequency. For an open-loop system the output consists of the following elements:

$$\underline{Y}(k) = \underline{G}_{\text{BLA}}(\omega_k)\underline{U}(k) + \underline{\mathcal{T}}_G(\omega_k) + \underline{H}(\omega_k)\underline{E}(k) + \underline{\mathcal{T}}_H(\omega_k). \tag{4}$$

Where $\underline{\mathcal{T}}_G$ and $\underline{\mathcal{T}}_H$ are the transients originating from the (assumed to be linear) plant and the noise respectively, $\underline{H}$ is the noise filter and $\underline{E}$ the frequency representation of the noise. Both transient contributions can be estimated by one term, hence (4) is rewritten into:

$$\underline{Y}(k) = \underline{G}_{\text{BLA}}(\omega_k)\underline{U}(k) + \underline{\mathcal{T}}(\omega_k) + \underline{V}(k), \tag{5}$$

in which $\underline{\mathcal{T}} = \underline{\mathcal{T}}_G + \underline{\mathcal{T}}_H$ and $\underline{V}$ is a residual caused by disturbances such as measurement noise. Before estimating the BLA of the plant, the transient $\underline{\mathcal{T}}$ is approximated and removed from the data.

Transient estimation   The transient calculation hinges on the existence of unexcited frequencies. At these detection lines the input caries no power, hence for the output this yields:

$$\underline{Y}(k + r_P) = \underline{\mathcal{T}}(\omega_{k+r_P}) + \underline{V}(k + r_P). \tag{6}$$

Where r_P is a vector which contains surrounding unexcited frequencies of an excitation line k.

For a SISO system, the transient of the output is estimated by a rational function:

$$\mathcal{T}(\omega_{k+r_P}) = \frac{N_{\mathcal{T}}(\omega_{k+r_P})}{D_{\mathcal{T}}(\omega_{k+r_P})} = \frac{\sum_{s=0}^{n_{\mathcal{T}}} t_s(k)r_P^s}{1 + \sum_{s=1}^{n_D} d_s(k)r_P^s}. \tag{7}$$

With the numerator and denominator polynomials of respective orders $n_{\mathcal{T}}$ and n_D. Where, t_s and d_s are the polynomial coefficients corresponding to order s. The coefficient of order 0 of the denominator polynomial is chosen as 1. Hence, the estimation of the rational function becomes linear in the parameters. Substitution of (7) in (6) yields:

$$D_{\mathcal{T}}(\omega_{k+r_P})Y(k + r_P) =$$
$$N_{\mathcal{T}}(\omega_{k+r_P}) + D_{\mathcal{T}}(\omega_{k+r_P})V(k + r_P). \tag{8}$$

Now, substituting the polynomial expansion given in (7) into (8) gives rise to an expression that is linearly depending on the polynomial coefficients of the transient.

$$Y(k + r_P) = \sum_{s=0}^{n_{\mathcal{T}}} t_s(k)r_P^s - Y(k + r_P)\sum_{s=1}^{n_D} d_s(k)r_P^s +$$
$$V(k + r_P)\left(1 + \sum_{s=1}^{n_D} d_s(k)r_P^s\right). \tag{9}$$

This approach can be extended to a MIMO framework, where the transient estimations for all N_y outputs are concatenated and rewritten into the form of:

$$\underline{Y}(k + r_P) = \Theta_{\mathcal{T}}K_{\mathcal{T}}(k + r_P) + \underline{V}(k + r_P), \tag{10}$$

which yields a linear set of equations where $\Theta_{\mathcal{T}}$ contains the polynomial coefficients and $K_{\mathcal{T}}$ the corresponding linear dependencies. These matrices are of dimensions: $\underline{Y} \in \mathbb{R}^{(N_y)\times(2(N_P-1))}$, $\Theta_{\mathcal{T}} \in \mathbb{R}^{(N_y)\times(1+n_{\mathcal{T}}+N_y n_D)}$, and $K_{\mathcal{T}} \in \mathbb{R}^{(1+n_{\mathcal{T}}+N_y n_D)\times(2(N_P-1))}$.

By transposing (10), $\Theta_{\mathcal{T}}$ can be computed at frequency bin k according to solving the system $\underline{A}x = \underline{b}$, where x contains the unknown parameters. This yields the least squares fit of the rational function over the frequency window r_P that minimizes the residual term $\underline{V}$ according to:

$$\hat{\Theta}_{\mathcal{T}} = \arg\min_{\Theta_{\mathcal{T}}} \sum_{r \in r_P} |\underline{Y}(k + r) - \underline{\mathcal{T}}(\omega_{k+r})|^2. \tag{11}$$

The transient estimation at frequency k for every transfer is then given by the first column of $\hat{\Theta}_{\mathcal{T}}$, which contains N_y elements corresponding to the N_y transients. Next, the transient-free output can be constructed according to:

$$\hat{\underline{Y}}(k) = \underline{Y}(kN_P) - \underline{\mathcal{T}}(k). \tag{12}$$

Computing the best linear approximation   The BLA of the plant is based on the transient-free output $\hat{\underline{Y}}$ which only contains information of the excited frequencies. Due to the removal of the transient, (5) reduces to:

$$\hat{\underline{Y}}(k + r_E) = \underline{G}_{\text{BLA}}(\omega_{k+r_E})\underline{U}(k + r_E) + \underline{V}(k + r_E). \tag{13}$$

The LRM is applied once more on the transient-free data to estimate the system response at every excited frequency. Therefore, a rational function is now fitted on a set of r_E adjacent excited frequencies

$$r_E = [-N_E, -N_E + 1, \ldots, 0, \ldots, N_E - 1, N_E], \tag{14}$$

where N_E is a user defined number of frequencies that determines the size of the estimation window. For a SISO system, the rational function that estimates the BLA is similar to the transient estimation (7):

$$G_{\text{BLA}}(\omega_{k+r_E}) = \frac{N_G(\omega_{k+r_E})}{D_G(\omega_{k+r_E})} = \frac{\sum_{s=0}^{n_G} g_s(k)r_E^s}{1 + \sum_{s=1}^{n_D} d_s(k)r_E^s}, \tag{15}$$

in which the numerator and denominator polynomials are of order n_G and n_D, respectively.

However, due to the dependency on the input, substituting (15) in (13) yields a different result with respect to the transient case, i.e.,

$$D_G(\omega_{k+r_E})\hat{Y}(k+r_E) = N_G(\omega_{k+r_E})\underline{U}(k+r_E)+$$
$$D_G(\omega_{k+r_E})V(k+r_E). \quad (16)$$

Further substitution of the polynomial expansion in (15) leads to an expression with linear dependencies on the polynomial coefficients:

$$\hat{Y}(k+r_E) = U(k+r_E)\sum_{s=0}^{n_G} g_s(k)r_E^s -$$
$$\hat{Y}(k+r_E)\sum_{s=1}^{n_D} d_s(k)r_E^s + V(k+r_E)\left(1+\sum_{s=1}^{n_D} d_s(k)r_E^s\right). \quad (17)$$

Yet again, extending this to a MIMO framework and concatenating the resulting $N_y N_u$ equations leads to the system of equations given by

$$\underline{\hat{Y}}(k+r_E) = \Theta_G K_G(k+r_E) + \underline{V}(k+r_E). \quad (18)$$

These matrices are of dimensions: $\underline{\hat{Y}} \in \mathbb{R}^{(N_y)\times(2N_E+1)}$, $\Theta_G \in \mathbb{R}^{(N_y)\times(N_u(n_G+1)+N_y n_D)}$, and $K_G \in \mathbb{R}^{(N_u(n_G+1)+N_y n_D)\times(2N_E+1)}$.

Matrix Θ_G can be computed from the transposed description similar to (10). The matrix K_G is scaled by its 2-norm again according to (Pintelon and Schoukens, 2012, Section 7.2.2.5) such that the calculations are numerically stable. This yields the least squares fit of the rational function over the frequency window r_E that minimizes the residual term $\underline{V}$ according to (19).

$$\hat{\Theta}_G = \arg\min_{\Theta_G} \sum_{r=-N_E}^{N_E} |\underline{\hat{Y}}(k+r) - \underline{G}_{\text{BLA}}(\omega_{k+r})\underline{U}(k+r)|^2. \quad (19)$$

The BLA elements at frequency k can be found in the first N_u columns of the N_y rows in $\hat{\Theta}_G$. However, since the LRM depends on a window of N_E frequency bins adjoining k, $\hat{\Theta}_G$ can only be estimated for $k \in [N_E+1, N_k-N_E]$. It is, however, possible to obtain an approximation at frequencies outside of $k \in [N_E+1, N_k-N_E]$ by the use of an asymmetric windowing function, i.e. where the estimated frequency is no longer at the center of the window and the rational function is fitted on an asymmetric domain.

4. PARAMETRIC IDENTIFICATION

The goal of the considered algorithm is to compute a parametric model that captures the behaviour of the available frequency response data as accurately as possible, especially in control relevant frequency regions. The algorithm strives towards minimization of the difference between the obtained parametric model and the non-parametric estimate in an $\mathcal{H}_\infty$-norm sense.

The identification procedure revolves around a control-relevant approach, similar to (Oomen et al., 2014), in which the $\mathcal{H}_\infty$-norm based criterion $\mathcal{J}(P,C)$ in (20) is the objective for minimization

$$\mathcal{J}(P,C) = \|WT(P,C)V\|_\infty. \quad (20)$$

Here, P is a multivariable plant, C is a controller, W and V are weighting functions, and $T(P,C)$, given in (21),

Fig. 2. General feedback configuration appended with weighting functions.

consists of the closed-loop transfers of the signals that are depicted in Figure 2.

$$T(P,C) : \begin{bmatrix} r_2 \\ r_1 \end{bmatrix} \mapsto \begin{bmatrix} y \\ u \end{bmatrix} = \begin{bmatrix} P \\ I \end{bmatrix} (I+CP)^{-1} [C\ I]. \quad (21)$$

As (20) depends on both the plant and the controller, this criterion should be minimized through both of them. This aids the goal of finding an optimal controller for the closed-loop objectives specified by the weighting functions. This duality is a key feature of the control-relevant identification procedure. Considering again (20), the optimal controller is defined by:

$$C^{\text{opt}} = \arg\min_C \mathcal{J}(P_o, C), \quad (22)$$

in which P_o is the true plant. However, since P_o is not known beforehand, a non-optimal experimental controller C^{exp} is designed that stabilizes a non-parametric plant estimate G.

Applying the triangle inequality to (20) yields a relation of the closed-loop performance of any candidate model P with respect to the real system, see Oomen et al. (2014):

$$\mathcal{J}(P_o, C) \leq \mathcal{J}(P, C) + \|W(T(P_o, C) - T(P, C))V\|_\infty. \quad (23)$$

If this expression is evaluated for the experimental controller and minimized over P, the control-relevant identification criterion for the nominal plant $\hat{P}$ becomes:

$$\hat{P} = \arg\min_P \|W(T(P_o, C^{\text{exp}}) - T(P, C^{\text{exp}}))V\|_\infty. \quad (24)$$

Hence, the resulting $\hat{P}$ is evaluated with respect to the closed-loop control objectives specified in the weighting functions W and V. Again P_o is unknown, but it can be substituted by a measured non-parametric frequency response estimate G, which is assumed to approximate P_o.

The nominal model is internally structured as a factorization of two coprime factors, i.e., $\hat{P} = \hat{N}\hat{D}^{-1}$. The coprime structure enables the identification of common dynamics, which aids the identification of models with a low McMillan degree. This factorization can be exploited to recast the nominal plant identification of (24) into a coprime factor identification problem, see Oomen et al. (2014); Oomen and Bosgra (2012):

$$\min_{\hat{N},\hat{D}} \left\|W\left(\begin{bmatrix} N_o \\ D_o \end{bmatrix} - \begin{bmatrix} \hat{N} \\ \hat{D} \end{bmatrix}\right)\widetilde{N}_e\right\|_\infty, \quad (25)$$

where $\{N_o, D_o\}$ represents the right coprime factorization of P_o and $\widetilde{N}_e$ is part of the left coprime factorization $\{\widetilde{N}_e, \widetilde{D}_e\}$ of $[C^{\text{exp}}V_2\ V_1]$ that uniquely connects the control-relevant identification to the identification of coprime factors. The nominal and true plant are factorized according to:

$$\begin{bmatrix} N \\ D \end{bmatrix} = \begin{bmatrix} P \\ I \end{bmatrix}(\widetilde{D}_e + \widetilde{N}_{e,2}V_2^{-1}P)^{-1}, \quad (26)$$

with $\widetilde{N}_e = \begin{bmatrix} \widetilde{N}_{e,1} & \widetilde{N}_{e,2} \end{bmatrix}$. Furthermore, $\widetilde{N}_e$ is factorized as a co-inner function Oomen et al. (2014) and as such does not influence the $\mathcal{H}_\infty$-norm in (25). Hence, it can be removed from this expression.

To arrive at a solvable identification problem, the $\mathcal{H}_\infty$-norm in (25) is rewritten into its frequency domain interpretation (with $\widetilde{N}_e$ removed):

$$\min_{\hat{N},\hat{D}} \ \max_{\omega_i \in \Omega^{\mathrm{id}}} \ \bar{\sigma}\left(W\left(\begin{bmatrix} N_o \\ D_o \end{bmatrix} - \begin{bmatrix} \hat{N} \\ \hat{D} \end{bmatrix}\right)\right), \qquad (27)$$

where Ω^{id} contains the identified frequencies and $\bar{\sigma}$ indicates the maximum singular value of the expression evaluated at a certain $\omega_i \in \Omega^{\mathrm{id}}$. Furthermore, the non-parametric estimates of the factors of the true plant are defined as:

$$\begin{bmatrix} \widetilde{N}_o \\ \widetilde{D}_o \end{bmatrix} = \widetilde{T}(P_o, C^{exp})V\widetilde{N}_e^H \ \text{ for } \omega_i \in \Omega^{\mathrm{id}}. \qquad (28)$$

The optimal nominal model $\{\hat{N}, \hat{D}\}$ can be obtained through a specific parametrization according to:

$$\begin{bmatrix} \hat{N}(\theta) \\ \hat{D}(\theta) \end{bmatrix} = \begin{bmatrix} B(\theta) \\ A(\theta) \end{bmatrix} \left(\widetilde{D}_e A(\theta) + \widetilde{N}_{e,2}V_2^{-1}B(\theta)\right)^{-1}. \qquad (29)$$

Here, A and B are polynomial matrices and θ indicates the vector of unknown parameters. The corresponding multivariable parametrization of $\hat{P}$ is then given by:

$$\hat{P}(\theta) = \hat{N}(\theta)\hat{D}(\theta)^{-1} = B(\theta)A(\theta)^{-1}. \qquad (30)$$

Wherein the dynamics introduced into B and A by the experimental controller $C^{\exp}$ and the weighting functions V_1 and V_2 cancel each other out. Hence, the nominal plant $\hat{P}$ is obtained, which, due to its parametrization as a matrix fraction description, can take common dynamics between the inputs and outputs into account. This yields a model with a low McMillan degree.

In order to minimize (27), which is a nonsmooth optimization problem due to the discrete frequency grid, the Lawson algorithm is employed as described in (Oomen and Bosgra, 2012, Section VI). The Lawson algorithm appends (27) with a frequency dependent weighting function that adapts itself every iteration based on the modeling error.

Computing the parameter vector θ corresponding to the coprime factorization that minimizes (27) is a non-convex optimization problem because the parametrization given in (29) is nonlinear in the parameters θ. An initial estimate for θ is computed using the Sanathanan-Koerner (SK) iterative weighted linear least squares algorithm (Oomen et al., 2014)(Pintelon and Schoukens, 2012, Section 9.8.3). The SK iterations typically converge close to the globally optimal solution. This remarkable property arises from the fact that it does not search the error surface as is the case for most common optimization routines. However, the SK-algorithm usually does not converge exactly to the global optimum due to undermodeling and noise (Oomen and Bosgra, 2012). Therefore, to further refine the estimate of the parameter vector θ, it is succeeded by a Gauss-Newton optimization.

5. EXPERIMENTAL RESULTS

5.1 Non-parametric identification results

To identify a robust BLA of the 2-input 2-output plant, $N_M = 13$ realisations of the multisine excitation are measured and consequently 26 experiments are executed.
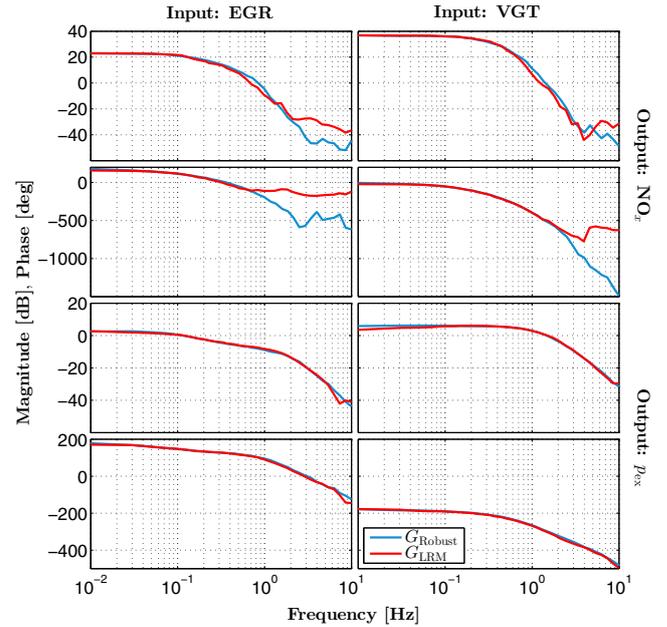

Fig. 3. LRM BLA estimation in comparison with the robust BLA estimation.

The input signal is designed according to the discussion in Section 3.1. The system is allowed to settle into a steady state for one minute after the initial excitation is applied in order to get rid of transient behaviour. Thereafter, multisines of period $T = 100$ s are measured for $N_P = 6$ consecutive periods per experiment.

To test the performance of the fast LRM method another identification experiment is performed and the results are compared to the robust BLA. The system is excited for $N_P = 6$ periods. However, no measures are taken to eliminate transient effects from the data as the LRM method should be able to cope with these effects. Empirically, it is determined that the polynomial orders $n_{\mathcal{T}} = 2$, $n_G = 2$ and $n_D = 2$ yield the best BLA estimates. These relatively low orders provide a good fit due to the absence of lowly damped behaviour. The frequency bin width of the LRM estimation window N_E is set to 8.

The LRM estimation is close to the measured BLA using the robust method, considering the severe reduction in measurement time (1 experiment as opposed to 26 experiments). The magnitude and phase of the plant elements corresponding with the output exhaust manifold pressure p_{ex} are estimated accurately. The NO_x output elements show larger deviations from the robust BLA estimation, especially for higher frequencies ($f > 1$ Hz) which could be caused by the limited signal to noise ratio.

5.2 Parametric identification results

The McMillan degree of the identified coprime factors depend on the McMillan degree of the experimental controller $C^{\exp}$ and weighting filters (Oomen and Bosgra, 2012). Thus, a low complexity controller will enable accurate identification of low order models. The control design of (Criens et al., 2015) based on static decoupling with decentralized PI control is adopted to serve as experimental controller in the fitting procedure.

The non-parametric identification experiments indicate that the plant contains delays in certain input-output
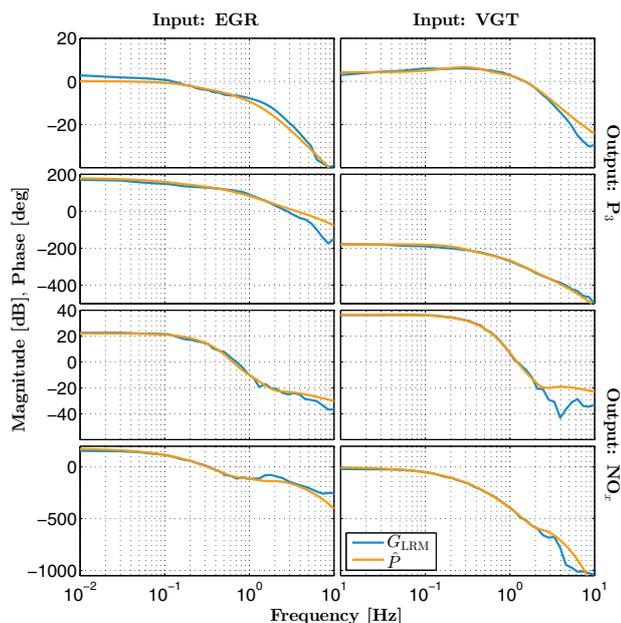
Fig. 4. Bode plot of the LRM estimate based on 3 multisine periods of 100s and the parametric model fit.

channels. The parametric fitting procedure is not capable of identifying these delays and thus the behaviour introduced by them will hinder the resulting model quality. Therefore, it is desired to estimate the delays and remove them before the fitting procedure. This results in a parametric fit of the approximate delay-free system. After fitting, the estimated delays are added back into the model.

The parametric 6th order state space model is shown in Figure 4. Although the parametric fit is not accurate on the full domain of identified frequencies, it can be observed that in the frequency range of 0.2 to 1 Hz the identified dynamics are captured accurately. This frequency range encompasses the expected bandwidth of the system, i.e. the crossover region of the shaped system. The high accuracy in the control-relevant frequency region is a direct result from the evaluation of the parametric model with respect to closed-loop control objectives. The parametrization of the multivariable nominal plant is computed according to (30).

6. CONCLUSION AND OUTLOOK

An accurate non-parametric and parametric identification procedure for heavy-duty diesel engines is presented which exceeds the present state-of-the-art in terms of required measurement time and model complexity. The fast LRM provides an efficient way to obtain local linear system descriptions. Subsequently, parametric models with a low McMillan degree are identified for a 2x2 engine model with high accuracy in control-relevant frequency regions. This renders the identified model particularly useful for model-based control design which is presently pursued.

REFERENCES

Broomhead, T., Manzie, C., Shekhar, R., Brear, M., and Hield, P. (2014). Robust stable economic mpc with applications in engine control. *IEEE Conference on Decision and Control*, 2511–2516.

Calendini, P. and Breuer, S. (2010). Mean value engine models applied to control system design and validation.

In L. del Re, F. Allgöwer, L. Glielmo, C. Guardiola, and I. Kolmanovsky (eds.), *Automotive Model Predictive Control*, chapter 3. Springer-Verlag London.

Criens, C., van Keulen, T., Willems, F., and Steinbuch, M. (2016). A control oriented multivariable identification procedure for turbocharged diesel engines. *International Journal of Powertrains*, 5(2), 95–119.

Criens, C., Willems, F., van Keulen, T., and Steinbuch, M. (2015). Disturbance rejection in diesel engines for low emissions and high fuel efficiency. *IEEE Transactions on Control Systems Technology*, 23(2), 662–669.

Eriksson, L. and Nielson, L. (2014). *Modeling and Control of Engines and Drivelines*. John Wiley & Sons, Ltd, 1st edition.

Gevers, M., Bombois, X., Codrons, B., Scorletti, G., and Anderson, B. (2003). Model validation for control and controller validation in a prediction error identification framework-part i: Theory. *Automatica*, 39(3), 403–415.

Guardiola, C., Gil, A., Pla, B., and Piqueras, P. (2012). Representation limits of mean value engine models. In D. Alberer, H. Hjalmarsson, and L. del Re (eds.), *Identification for Automotive Systems*, chapter 11. Springer-Verlag London.

Henningsson, M., Ekholm, K., Strandh, P., Tunestål, P., and Johansson, R. (2012). *Dynamic mapping of diesel engine through system identification*. Springer, in d. alberer, h. hjalmarsson, and l. del re, editors, identification for automotive systems edition.

Isermann, R. (2014). *Engine modeling and control*. Springer, Berlin, 1st edition.

Karlsson, M., Ekholm, K., Strandh, P., Johansson, R., and Tunestål, P. (2010). Multiple-input multiple-output model predictive control of a diesel engine. *6th IFAC Symp. Advances in Automotive Control*, 1, 131–136.

McKelvey, T. and Guérin, G. (2012). Non-parametric frequency response estimation using a local rational model. *IFAC Symposium on System Identification*, 16(1), 49–54.

Oomen, T. and Bosgra, O. (2012). System identification for achieving robust performance. *Automatica*, 48(9), 1975–1987.

Oomen, T., van Herpen, R., Quist, S., van de Wal, M., Bosgra, O., and Steinbuch, M. (2014). Connecting system identification and robust control for next-generation motion control of a wafer stage. *IEEE Transactions on Control Systems Technology*, 22(1), 102–118.

Pintelon, R. and Schoukens, J. (2012). *System Identification: A Frequency Domain Approach*. Wiley-IEEE Press.

Schoukens, J., Vaes, M., and Pintelon, R. (2016). Linear system identification in a nonlinear setting. *IEEE Control Systems Magazine*, 36(3), 38–69.

Sharma, R., Nesic, D., and Manzie, C. (2011). Model reduction of turbocharged (tc) spark ignition (si) engines. *Transactions on Control Systems Technology*, 19, 297–310.

Stewart, G., Borrelli, F., Pekar, J., Germann, D., Pachner, D., and Kihas, D. (2010). Toward a systematic design for turbocharged engine control. In L. del Re, F. Allgöwer, L. Glielmo, C. Guardiola, and I. Kolmanovsky (eds.), *Automotive Model Predictive Control*, chapter 14. Springer-Verlag London.

Wang, X., Waschl, H., Alberer, D., and del Re, L. (2011). A design framework for predictive engine control. *Oil & Gas Science and Technology - Rev. IFP Energies nouvelles*, 66(4), 599–612.